



ELSEVIER

Journal of Crystal Growth 240 (2002) 463–466

JOURNAL OF  
**CRYSTAL  
GROWTH**

www.elsevier.com/locate/jcrysgr

# High intense UV-luminescence of nanocrystalline ZnO thin films prepared by thermal oxidation of ZnS thin films

X.T. Zhang, Y.C. Liu\*, Z.Z. Zhi, J.Y. Zhang, Y.M. Lu, W. Xu, D.Z. Shen,  
G.Z. Zhong, X.W. Fan, X.G. Kong

*Changchun Institute of Optics, Fine Mechanics and Physics Key Laboratory of Excited State Processes,  
Chinese Academy of Science, 1-Yan An Road, 130021 Changchun, China*

Received 21 September 2001; accepted 10 February 2002

Communicated by R. James

## Abstract

High quality zinc oxide (ZnO) films were obtained by thermal oxidation of high quality ZnS films. The ZnS films were deposited on a Si substrate by a low-pressure metalorganic chemical vapor deposition technique. X-ray diffraction spectra indicate that high quality ZnO films possessing a polycrystalline hexagonal wurtzite structure with preferred orientation of (002) were obtained. A fourth order LO Raman scattering was observed in the films. In photoluminescence (PL) measurements, a strong PL with a full-width at half-maximum of 10 nm around 380 nm was obtained for the samples annealed at 900°C at room temperature. The maximum PL intensity ratio of the UV emission to the deep-level emission is 28 at room temperature, providing evidence of the high quality of the nanocrystalline ZnO films. © 2002 Published by Elsevier Science B.V.

*PACS:* 78.55.Et; 78.30.Fs; 81.05.Dz; 81.07.Bc; 82.33.Ya

*Keywords:* A1. Nanostructures; A1. Photoluminescence; A1. X-ray diffraction; A3. Low press metalorganic vapor phase epitaxy; B1. Zinc compounds; B2. Semiconducting II–VI materials

## 1. Introduction

Zinc oxide (ZnO) is an interesting wide band gap semiconductor material with a direct band gap of 3.37 eV at room temperature and exciton binding energy of 60 meV. It attracts much attention because of its potential device applications [1–3]. The photoluminescence (PL) spectra of ZnO thin films show a near band edge (NBE) UV

emission and a defect-related deep level (DL) emission. The DL emissions are usually related to structural defects and impurities. All structural defects originate from an insufficient supply of oxygen during growth. In order to prepare a high quality ZnO thin film, it is necessary to minimize structural defects.

Assuming that ZnO can be grown on Si substrates, ZnO on Si offers an interesting opportunity for various properties of ZnO to be combined with advanced Si electronics. Direct growth of epitaxial ZnO films on Si, however, is known to be an extremely difficult task when using

\*Corresponding author. Tel.: +86-431-5937596; fax: +86-431-5955378.

*E-mail address:* ycliu@nenu.edu.cn (Y.C. Liu).

either the metalorganic chemical vapor deposition (MOCVD) or molecular beam epitaxy (MBE) technique, because the oxygen ( $O_2$ ) used in the experiment easily oxidizes the organic sources. Furthermore, to accurately control the flow rate of the  $O_2$  is a puzzling problem. One solution is to introduce enhanced oxygen plasma or pulsed laser deposition into the experiment [4,5]. As is well known, the successful growth of ZnS films on Si substrates using various growth techniques has been previously reported [6,7]. Additionally, the ZnS compound can be very easily oxidized to produce ZnO and the gas  $SO_2$ . In this paper, we present a useful and simple method for preparing nanocrystalline ZnO thin films with good NBE UV luminescent properties by thermal oxidation of high quality ZnS films.

## 2. Experiment

The ZnS thin films were grown on n-Si (100) substrates using dimethyl zinc (DMZn) and hydrogen sulfide ( $H_2S$ ) by the LP-MOCVD technique. The flow rates of DMZn,  $H_2S$ , and Hydrogen ( $H_2$ ) were fixed at  $28.65 \times 10^{-6}$  mol/min,  $4.00 \times 10^{-4}$  mol/min, and 1.31/min, respectively. The pressure of the growth chamber was 300 Torr. The films were deposited on n-Si (100) substrates, which were maintained at 320°C. The thickness of the deposited ZnS thin films was about 200 nm. After deposition, thermal oxidation of the films was carried out in an oxygen ambient at different temperature in the range 500–1000°C for 2 h. X-ray diffraction (XRD) spectra were measured. Raman spectrum measurements were carried out in a back-scattering geometry using a Micro-Raman spectrometer. A He–Cd laser with  $\lambda = 325$  nm was used as the excitation source for the resonant scattering studies. The PL was measured using the He–Cd laser operating at a wavelength of 325 nm.

## 3. Results and discussions

Fig. 1 shows the XRD patterns of ZnS thin films annealed at different temperatures ranging from

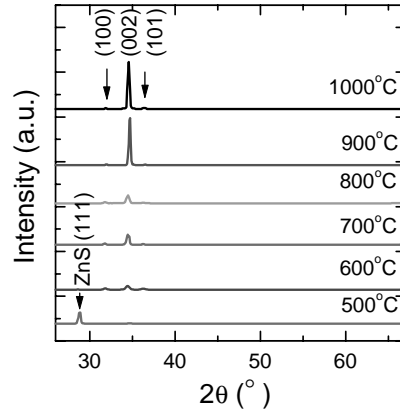


Fig. 1. XRD patterns of the ZnS films annealed at temperatures in the range 500–1000°C. Annealing temperatures are given in Fig. 1.

500°C to 1000°C. The XRD spectrum for an as-deposited ZnS thin film indicates that a high quality ZnS film with a cubic crystal structure has been obtained with a preferred (111) orientation (not shown in Fig. 1). When the films are annealed at 500°C, the XRD spectra show a mixed pattern of ZnS and ZnO peaks, indicating that the ZnS has begun a transformation from ZnS to ZnO. For the annealing temperature of 600°C, a (002) ZnO peak is clearly seen. For annealing temperatures  $T_a \geq 700^\circ\text{C}$ , the ZnS fully transforms into ZnO. The XRD patterns of the ZnO thin films indicate that they possess a polycrystalline hexagonal wurtzite structure with a preferential (002) orientation. As the annealing temperature increases, the diffraction peaks of the samples become sharper and more intense due to the increased particle size as well as the enhanced crystallinity. In order to evaluate the mean grain size of the films, the Scherrer's formula [8] was adopted. The mean grain sizes of the films are 20.04, 28.81, 38.41, 46.10, and 46.80 nm for the samples annealed at 600°C, 700°C, 800°C, 900°C, and 1000°C, respectively. High quality nanocrystalline ZnO thin films have been obtained.

Fig. 2 shows a representative room temperature Raman spectra of samples annealed at different temperatures. For comparison, the Raman spectrum for an as-deposited film is also shown in Fig. 2(a). The Raman spectrum of an as-deposited

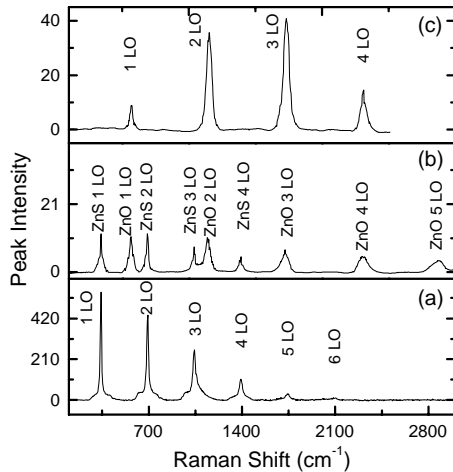


Fig. 2. Representative Raman spectra of the ZnS films annealed at different temperatures. (a) Shows the Raman spectrum for the as-deposited ZnS films, (b) and (c) show the Raman spectrum for the ZnS films annealed at a temperature of 600°C and 900°C, respectively.

film is composed of six sharp peaks. Multi-phonon processes of ZnS and ZnO lattices were observed in all the samples annealed at 600°C, indicating that ZnS has partly transformed into ZnO. This Raman spectrum consists of four sharp peaks, from ZnS, and five sharp peaks, from ZnO, as shown in Fig. 2(b). The Raman spectra of the ZnS lattice vibrations are multiples of the 1-LO zone-center frequency of  $349\text{ cm}^{-1}$ . It is smaller than the previously reported value of  $350\text{ cm}^{-1}$ . The Raman spectra of the ZnO lattice vibrations are multiples of the 1-LO ( $E_1$ ) zone-center frequency of  $574\text{ cm}^{-1}$ . It should be noted that the Raman scattering peaks of ZnS disappear at  $T_a = 700^\circ\text{C}$ , as shown in Fig. 2(c). This result is consistent with the XRD, indicating that the ZnS has fully converted to the ZnO phase. Meanwhile, the number of multiple phonon scattering processes observed in the semiconductor changes monotonically with the polaron coupling coefficient [9]. ZnO crystalline material has a large polaron coupling coefficient and large phonon frequency ( $574\text{ cm}^{-1}$ ), which results in enormous frequency shifts. Hence, the large 5-LO Raman shift indicates ZnO has a large deformation energy and implies that the films have good crystallinity. To

our knowledge, the multiple phonon-scattering processes were first observed in ZnO bulk crystalline material [10], but resonant Raman spectra in thin films, so far, have not been reported in the literature. The resonant Raman scattering has been previously discussed [11,12].

In the PL measurement, the main features of the PL spectra are similar for all samples annealed at different temperatures in the wavelength range 330–600 nm, and can be divided into two categories: the UV emission and the DL emission. As the annealing temperature increases from 600°C to 900°C, the UV PL intensity increases remarkably and the peaks become sharper. The strongest UV emission with the smallest full-width at half-maximum (FWHM) of 10 nm (or 88 meV) is seen around 380 nm for the films annealed at 900°C, as shown in Fig. 3. The DL emission band around 500 nm is barely observable. The crystallinity of the film gradually improves as the annealing temperature increases. At a sufficiently high annealing temperature, strain, due to distortion of the ZnO lattice during the transformation between ZnS ( $a = 5.405\text{ \AA}$ ) and ZnO ( $a = 3.0249\text{ \AA}$ ,  $c = 5.207\text{ \AA}$ ), is eliminated, and the structure defects in the ZnO lattice are distinctly decreased. When the annealing temperature, however, increases to  $T_a \geq 900^\circ\text{C}$ , the UV emission intensity begins to decrease, and the FWHM broadens, because some new defects, such

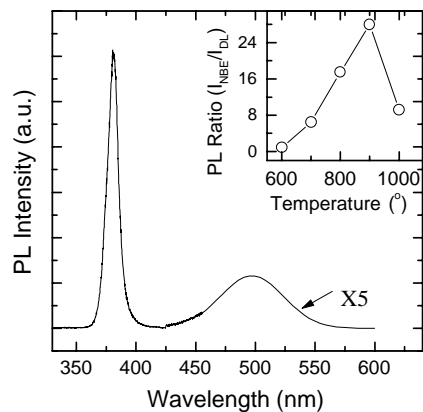


Fig. 3. The photoluminescence of the ZnS films annealed at 900°C. The inset shows the intensity ratio of the NBE emission to the DL emission for the samples annealed at different temperatures.

as oxygen vacancies and dangling bonds and so on, may be regenerated in the ZnO films at the higher annealing temperatures [13].

One way to evaluate the concentration of structural defects in ZnO films is to compare the PL intensity ratio of the UV emission to the DL green emission [4]. The reported epitaxial thin films grown by the MOCVD [14] technique showed relatively weaker DL emissions with a ratio of 1 at RT. In the case of bulk material, this ratio usually approaches zero as the temperature is raised to 295 K. In contrast, the largest ratio in our experiment is 28 at RT (see inset in Fig. 3). The FWHM of the samples annealed at 900°C is quite narrow, 10 nm (or 88 meV), compared with the 117 meV [4] observed for MBE-grown ZnO films at RT. The results of the PL spectra indicate the presence of strong exciton emissions with relatively weaker DL emissions. The concentrations of the defects responsible for the deep level emissions are relatively low. ZnO films prepared by thermal oxidation of ZnS thin films, prepared by MOCVD, appear to be composed of rather pure structure nearly defect-free ZnO polycrystalline material.

#### 4. Conclusion

We have obtained nanocrystalline ZnO films with a hexagonal wurtzite structure by thermal oxidation of high quality ZnS films. The LO phonon frequency shift for ZnO films is measured to be  $574\text{ cm}^{-1}$  by Raman spectroscopy. A strong UV emission is observed at room temperature for the samples annealed at 900°C. The maximum PL intensity ratio of UV emission to DL emission is 28 at RT.

#### Acknowledgements

This work was supported by the Program of CAS Hundred Talents, the National Natural Science Foundation of China, the Innovation Foundation of CIOFP, Excellent Young Teacher Foundation of Ministry of Education of China, and Jilin Distinguished Young Scholar Program.

#### References

- [1] D.M. Bagnall, Y.F. Chen, Z. Zhu, T. Yao, S. Koyama, M.Y. Shen, T. Goto, *Appl. Phys. Lett.* 70 (1997) 2230.
- [2] Z.K. Tang, G.K.L. Wong, P. Yu, M. Kawasaki, A. Ohtomo, H. Koinuma, Y. Segawa, *Appl. Phys. Lett.* 72 (1998) 3270.
- [3] H. Cao, Y.G. Zhao, H.C. Ong, S.T. Ho, J.Y. Dai, J.Y. Wu, R.P.H. Chang, *Appl. Phys. Lett.* 73 (1998) 3656.
- [4] Y. Chen, D.M. Bagnall, H.J. Koh, K.T. Park, K. Hiraga, Z. Zhu, T. Yao, *J. Appl. Phys.* 84 (1998) 3912.
- [5] R.D. Vispute, V. Talyansky, S. Chooun, R.P. Sharma, T. Venkatesan, M. He, X. Tang, J.B. Halpern, M.G. Spencer, Y.X. Li, G. Salamanca-Riba, A.A. Iliadis, K.A. Jones, *Appl. Phys. Lett.* 73 (1998) 348.
- [6] R.G. Benz, P.C. Hung, S.R. Stock, C.J. Summers, *J. Crystal Growth* 86 (1988) 303.
- [7] C. Giannini, T. Peluso, C. Gerardi, L. Tapfer, N. Lovergine, L. Vasanelli, *J. Appl. Phys.* 77 (1995) 2429.
- [8] B.D. Cullity, *Elements of X-ray Diffractions*, Addison-Wesley, Reading, MA, 1978, p. 102.
- [9] J.F. Scott, T.C. Damen, W.T. Silfvast, R.C.C. Leite, L.F. Cheesman, *Optics Commun.* 1 (1970) 397.
- [10] J.F. Scott, *Phys. Rev. B* 2 (1970) 1209.
- [11] J.F. Scott, R.C.C. Leite, T.C. Damen, *Phys. Rev.* 188 (1969) 1285.
- [12] D.C. Hamiton, *Phys. Rev.* 188 (1969) 1221.
- [13] H.J. Lozykowski, V.K. Shastri, *J. Appl. Phys.* 69 (1991) 3235.
- [14] S. Bethke, H. Pan, B.W. Wesseis, *Appl. Phys. Lett.* 52 (1988) 138.